Efficient and comprehensive EM field simulation procedure for pTX experiments

Frank Seifert[1], Tomasz Lindel[1], and Peter Ullmann[2]
[1]Physikalisch-Technische Bundesanstalt (PTB), Berlin, Germany, [2]Bruker BioSpin MRI GmbH, Ettlingen, Germany

Introduction and Motivation

Controlling local SAR is crucial for patient safety in parallel transmission (pTX) MRI. Electromagnetic (EM) field simulations based on FDTD or related methods are basic tools to determine multi-channel EM field distributions necessary for pTX RF pulse calculation and for predicting RF power deposition in the human body. A reliable simulation procedure should include realistic models of coil losses and actual matching and/or decoupling circuits. Thus, absolute validation, e.g. by B_1^+ and RF power measurements, should be feasible. Here, we present an efficient implementation of such a procedure based on post processing of FDTD data, i.e. complex valued E, H and J distributions for each channel in conjunction with the complex impedance matrix Z_{ij} calculated from steady state currents and voltages at the feeding ports of the coil array.

Materials and Methods

The applied simulation procedure consists of five steps as illustrated by an appropriate example – a cylindrical head phantom and a 4 channel CSA array (Fig.1) at 125 MHz [1]: (i) EM field calculation by FDTD: Using XFDTD 6.4 (Remcom Inc.) with a 2mm equidistant mesh of $8x10^6$ FDTD cells and current sources with CW excitation, complex valued 3D steady state E, H and J vector distributions were calculated driving each port consecutively. From port data the impedance matrix $Z_{ij} = U_i/I_j$ was calculated. Coil capacitors were adjusted to obtain $\mathrm{Im}[Z_{ii}] \approx 0$. This pre-tuning was kept fixed for all further calculations. (ii) Modeling of coil losses, matching circuits and coil coupling: For final tuning and matching to $Z_0 = 50\ \Omega$ a T-type matching circuit was used (consisting of Z_1, Z_2, Z_3) where $\mathrm{Re}[Z_1]$ was set to obtain the experimental value of $Q_{unloaded}/Q_{loaded} \approx 2$, whereas the imaginary parts of Z_1, Z_2 and Z_3 where determined by minimizing $\langle|S_{ii}|\rangle$ (average over all channels). For simplicity, the values for Z_1, Z_2, Z_3 were set equal for all channels (3 remaining parameters for optimization). Using the (symmetrical) head phantom individual $|S_{ii}|$ is better than -45 dB, when using a realistic in vivo head model (Duke from the Virtual Family, ITIS' Foundation) $|S_{ii}|$ values better than -22 dB can be achieved. As a result the complex valued coil currents are known when driving each coil element with unit voltage from a 50 Ω source. (iii) Calculation of field maps for the coupling coil array: Using the complex valued current amplitudes from step (ii) a linear superposition of all 3D field components was calculated for each driving port. Furthermore, B_1^+-maps where calculated for pTX RF pulse calculation. (iv) pTX RF pulse calculation: Using the simulated B_1^+-maps from step (iii) pTX RF pulses were calculated using the following parameters: spiral trajectory, 32 x 32 matrix, 4 channels, 2x acceleration, time step 10 µs, 496 time steps, target flip angle 45°, max. slew rate 200 mT/m/ms, max. gradient 40 mT/m. The target pattern is shown in Fig. 2.

Fig.1: Simulated phantom shell (Makrolon, $\sigma = 0.181$ mS/m, $\varepsilon = 2.9$) filled with phantom liquid ($\sigma = 0.33$ S/m, $\varepsilon = 76$). The 4 tubes are to support time-domain RF field probes.

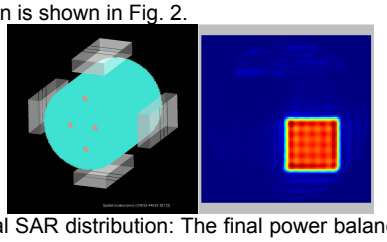

Fig.2: Simulated flip angle distribution for a off-centered rectangular target pattern (max. flip angle 45°) using simulated B_1^+-maps from the setup of Fig.1.

(v) Calculation of power balance and time averaged local SAR distribution: The final power balance and field superposition for each time step of the pTX RF pulse was calculated using the data from steps (i) to (iv). Instantaneous overall transmitter RF forward power $P_{Tx,forward}$, RF power absorbed by the phantom P_{abs} and RF power losses in the coil P_{coil} were calculated for each time step of the pTX pulse. Further, time averaged SAR (assuming a mass density of $1g/cm^3$) was calculated by subsequent temporal integration of instantaneous local SAR. Finally, the time averaged 3D SAR distribution was averaged over 10 cm^3 to obtain SAR_{10g} values. Steps (ii), (iii) and (v) were programmed in FORTRAN which can be easily adapted to GPU acceleration, 16 RF channels require > 10GB of RAM and 2 seconds computation time per field superposition (1 CPU core).

Results

Time courses of $P_{Tx,forward}$, P_{abs} and P_{coil} during the pTX pulse are shown in Fig.3. The peak power which is delivered by the RF amplifier system is about 220 W (for a 45° flip angle of the target pattern). In the average 43.3% of forward power is absorbed by the phantom, 33.8% is due to coil losses and 22.9% is absorbed by the RF amplifier (circulator). In Fig.4,5 maximum intensity projections of the time averaged local SAR distribution are shown. The tubes for RF field probes affect the SAR distribution slightly due to normal E-field components in off-centre positions. When calculating time averaged SAR_{10g} values the maximum value reach 5.6 W/kg. The ratio of maximum time averaged SAR_{10g} to time averaged forward RF power is 0.44/kg.

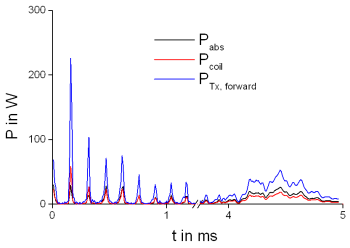

Fig.3: Time course of $P_{Tx,forward}$, P_{abs} and P_{coil} during pTX pulse of 4.96 ms duration

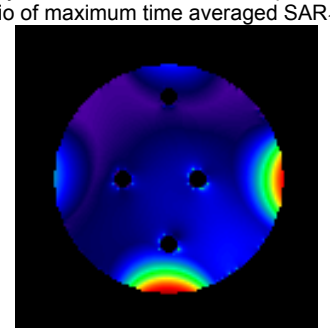

Fig.4: Calculated time averaged SAR (axial MIP), max. value 8.62 W/kg

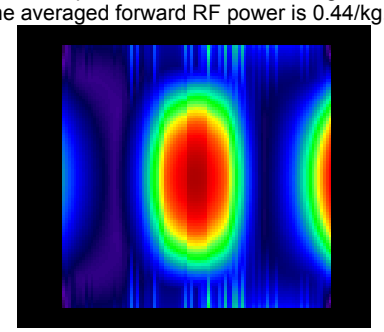

Fig.5: Calculated time averaged SAR (coronal MIP), max. value 8.62 W/kg

Using an efficient five step simulation procedure a complete and comprehensive calculation of all relevant parameters of a pTX experiment is feasible. The calculations include coil losses and matching circuits and are suitable for a absolute quantitative experimental validation using either B_1^+-maps or data from time-domain field probes.

This work is a part of the INUMAC project supported by the German Federal Ministry of Education and Research, grant #13N9207.

[1] F. Seifert, G. Wuebbeler, S. Junge, B. Ittermann, and H. Rinneberg, JMRI 26 (2007) 1315-1321